

Supplementary Materials for

Plasma from patients with bacterial sepsis or severe COVID-19 induces suppressive myeloid cell production from hematopoietic progenitors in vitro

Miguel Reyes *et al.*

*Corresponding author: Paul C. Blainey, pblainey@broadinstitute.org; Nir Hacohen, nhacohen@broadinstitute.org

Sci. Transl. Med. **13**, eabe9599 (2021)
DOI: 10.1126/scitranslmed.abe9599

The PDF file includes:

Figs. S1 to S11

Other Supplementary Material for this manuscript includes the following:

Tables S1 to S7
Data files S1 to S4

SUPPLEMENTARY FIGURES

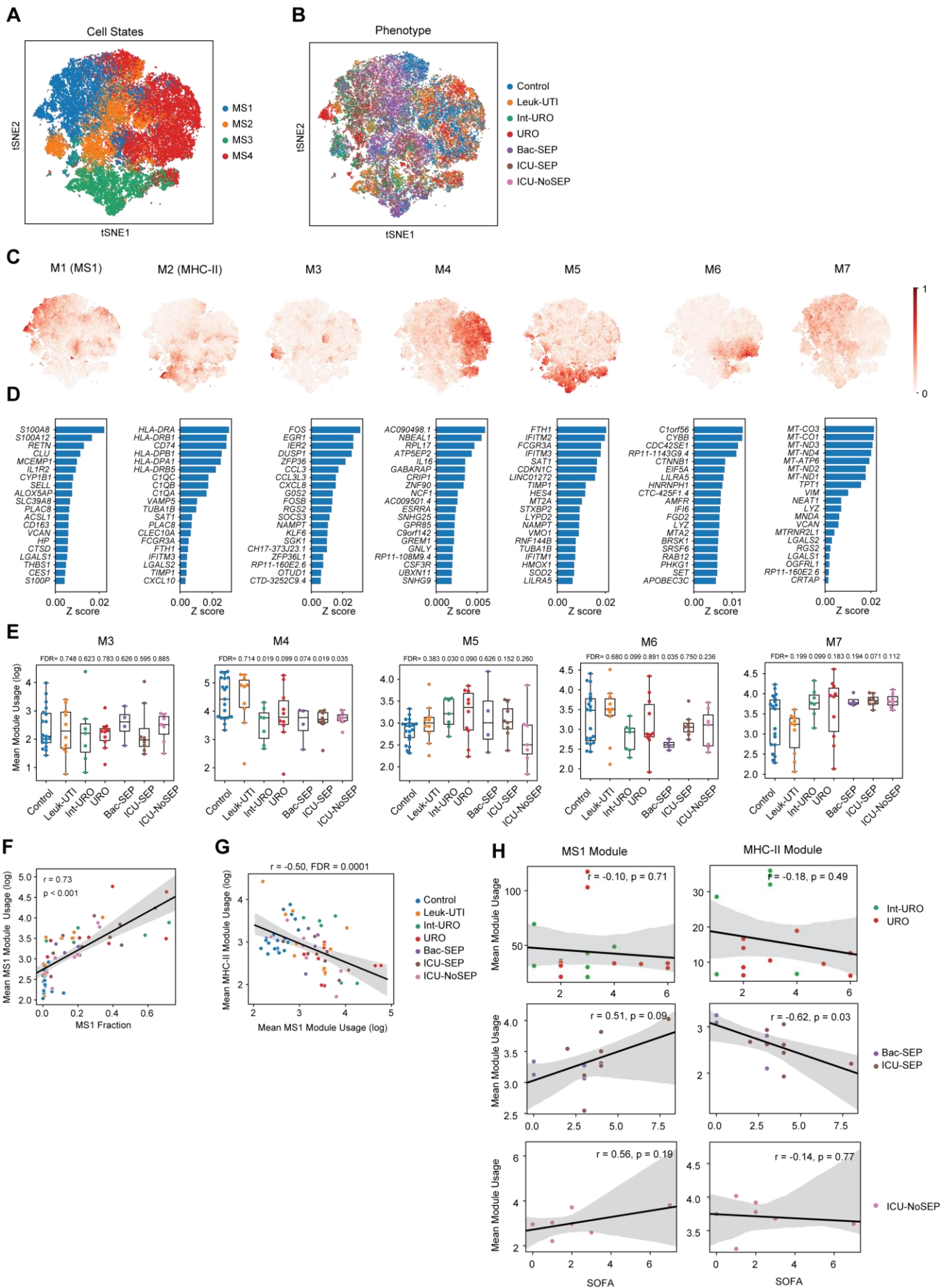


Figure S1. Characterization of gene expression modules in sepsis monocytes. (A-B) tSNE plot of monocytes from sepsis patients and controls colored by (A) cell state and (B) cohort. (C) Relative usage of gene expression module unbiasedly derived from the monocyte scRNA-seq data. (D) Genes with the top 10 loading in each gene expression module. (E) Mean usage of each gene module in monocytes for each patient type. FDR values are shown when comparing each disease state with healthy controls (two-tailed Wilcoxon rank-sum test, corrected for testing of multiple modules). Boxes show the median and IQR for each patient cohort, with whiskers extending to 1.5 IQR in either direction from the top or bottom quartile. (F) Scatterplot showing correlation between mean MS1 gene module usage in monocytes and MS1 fractions for each patient. Line and shadow indicate linear regression fit and 95% confidence interval, respectively. Significance of the correlations (Pearson r) were calculated with a two-sided permutation test. (G) Scatterplot showing correlation between mean MS1 and MHC-II gene module usage in monocytes for each patient. Line and shadow indicate linear regression fit and 95% confidence interval, respectively. Significance of the correlations (Pearson r) were calculated with a two-sided permutation test and corrected for multiple comparison of modules. (H) Scatter plots showing the correlation between mean module usage in monocytes and SOFA scores for each subject. Line and shadow indicate linear regression fit and 95% confidence interval, respectively. Significance of the correlations (Pearson r) were calculated with a two-sided permutation test. Detailed description of the patient cohorts and number of cells and patient groups are outlined in Reyes, et al (23). Control, healthy controls; Leuk-UTI, urinary tract infection with leukocytosis; Int-URO, intermediate urosepsis; URO, urosepsis; Bac-SEP, sepsis with confirmed bacteremia; ICU-SEP, intensive care with sepsis; ICU-NoSEP, intensive care without sepsis; SOFA, sequential organ failure assessment.

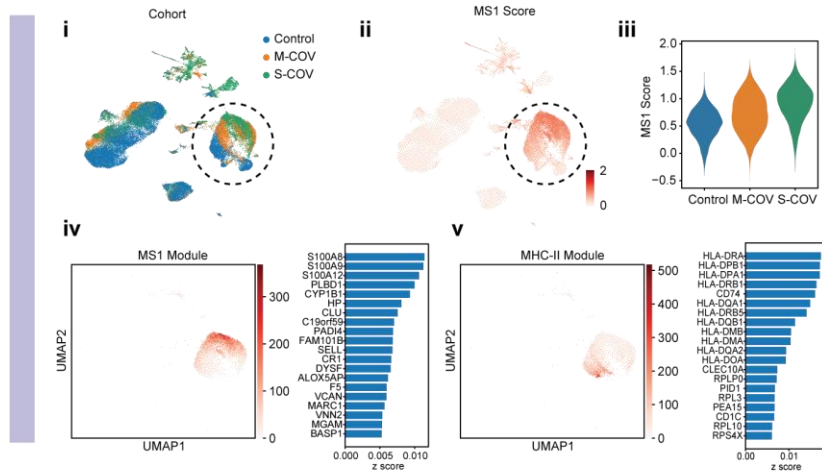
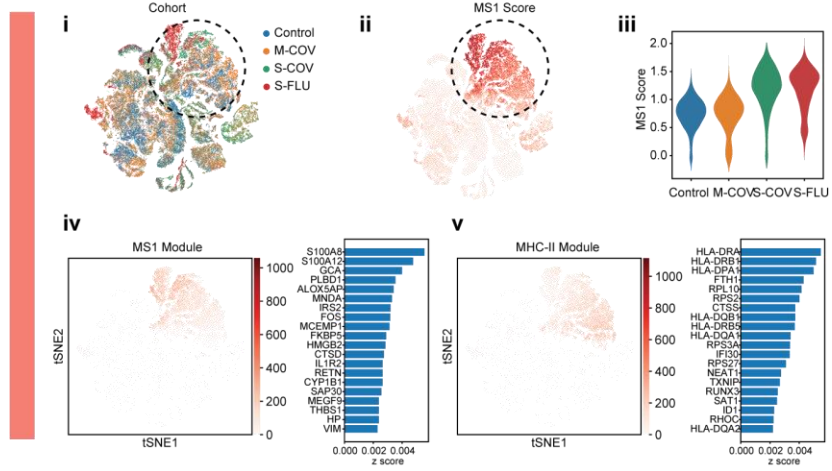
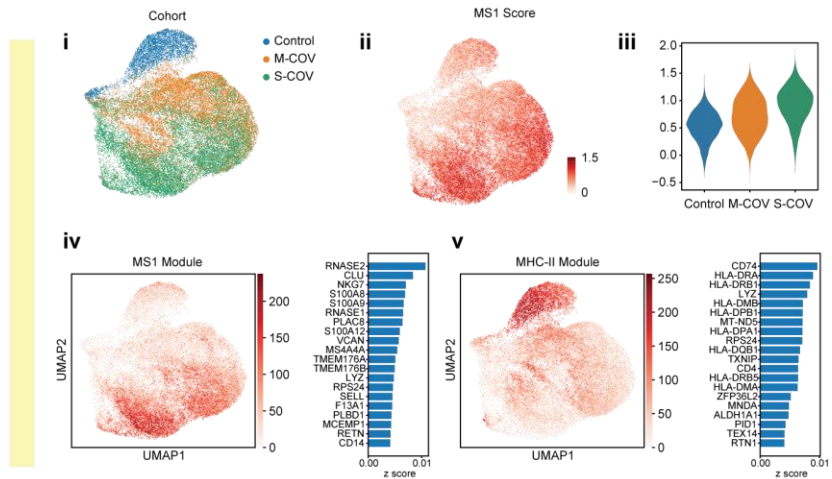
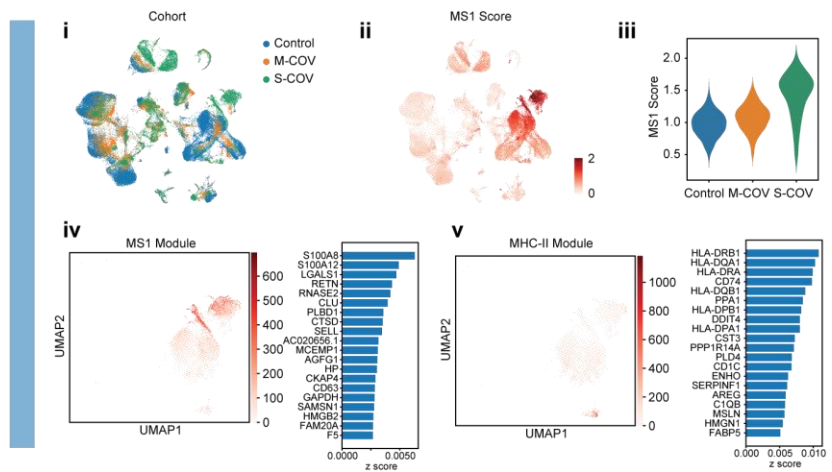
AWilk, *et al* 2020**B**Lee, *et al* 2020**C**Schulte-Schrepping, *et al* 2020**D**Arunachalam, *et al* 2020

Figure S2. Analysis of MS1 and MHC-II gene expression modules in COVID-19 blood scRNA-seq datasets. Independent analysis of four datasets: **(A)** Wilk, *et al* 2020, **(B)** Lee, *et al* 2020, **(C)** Schulte-Schrepping, *et al* 2020, and **(D)** Arunachalam, *et al* 2020. For each dataset: (i-ii) UMAP or tSNE projection of the cells colored by (i) patient condition and (ii) MS1 scores. (iii) Violin plot of MS1 scores for CD14-expressing cells from each condition. (iv-v) Left, UMAP or tSNE plot, showing usage of the MS1 and MHC-II gene expression modules unbiasedly derived from each dataset. Right, Barplots of the top 20 genes with the highest z-score loading in each module. Detailed description of the patient cohorts and number of cells and patients for each dataset in **(D,E)** are outlined in the corresponding publications (7, 28, 29, 31). M-COV, mild COVID-19; S-COV, severe COVID-19, S-FLU, severe influenza A.

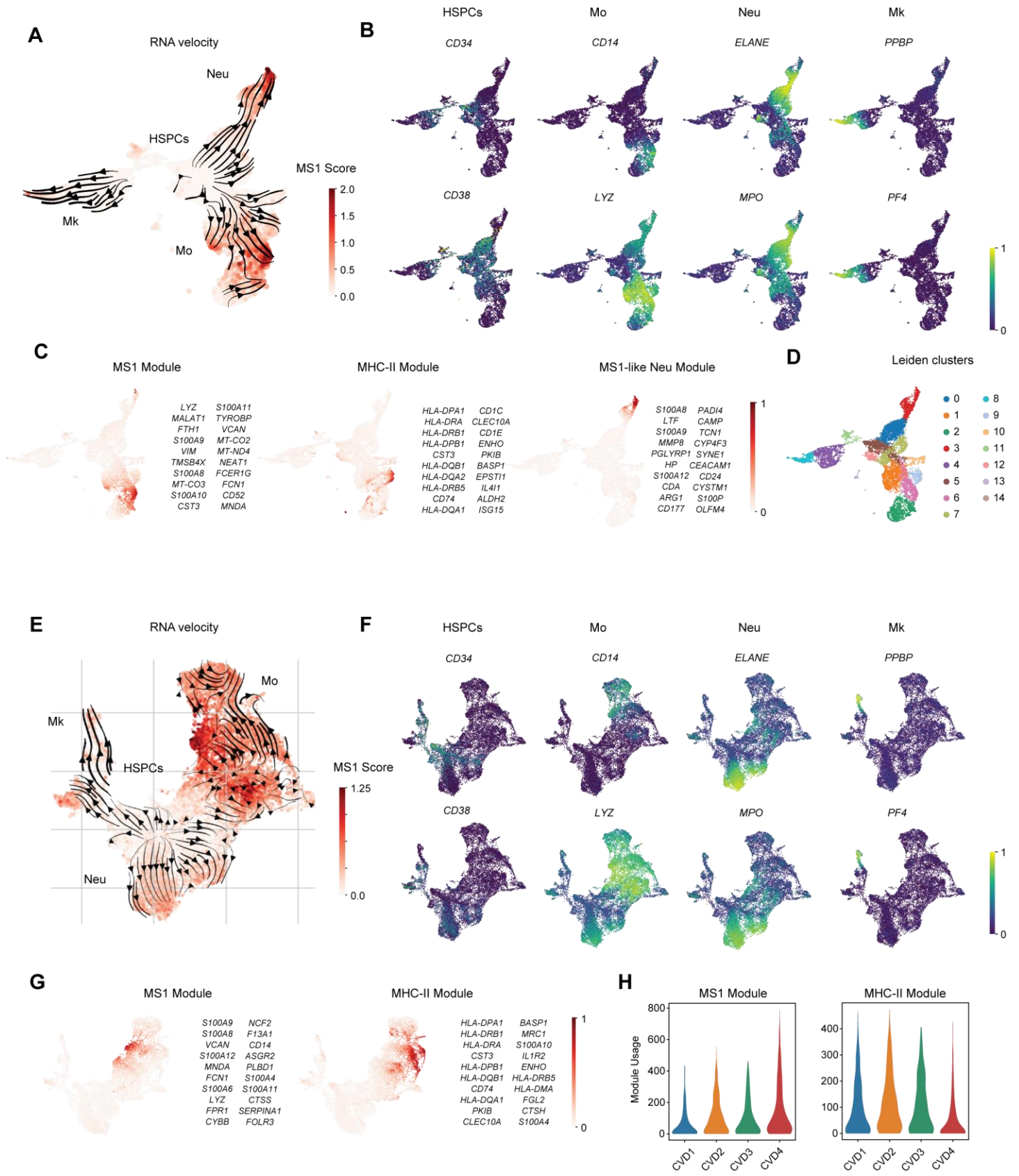


Figure S3. scRNA-seq of plasma-treated CD34+ HSPCs. (A-G) UMAP projection of differentiated cells from CD34+ HSPCs incubated with (A-D) sepsis or (E-G) COVID-19 plasma and corresponding controls. Cells are colored by (A,E) MS1 scores, (B,F) relative expression of HSPC, monocyte (Mo), neutrophil (Neu), and megakaryocyte (Mk) marker genes, (C,G) relative usage of the MS1 and MHC-II modules, and (d) Leiden clusters. Stream plots showing inferred trajectories from RNA velocity are overlaid in (A,E). Top 20 genes in each module are listed in (C,G). (H) Violin plots showing the usage of the MS1 (left) and MHC-II (right) modules in CD14-expressing cells across the different plasma treatment conditions. The experiment in (A-D) was performed on 2 healthy bone marrow donors with 2 plasma donors for each condition; a total of 3,039 and 5,254 cells were profiled for Control and URO plasma treatment, respectively. The experiment in (E-H) was performed on 2 healthy bone marrow donors with pooled plasma for each COVID-19 patient group; a total of 4,449, 4,591, 3,129 and 3,711 cells were profiled for CVD1-CVD4 plasma, respectively.

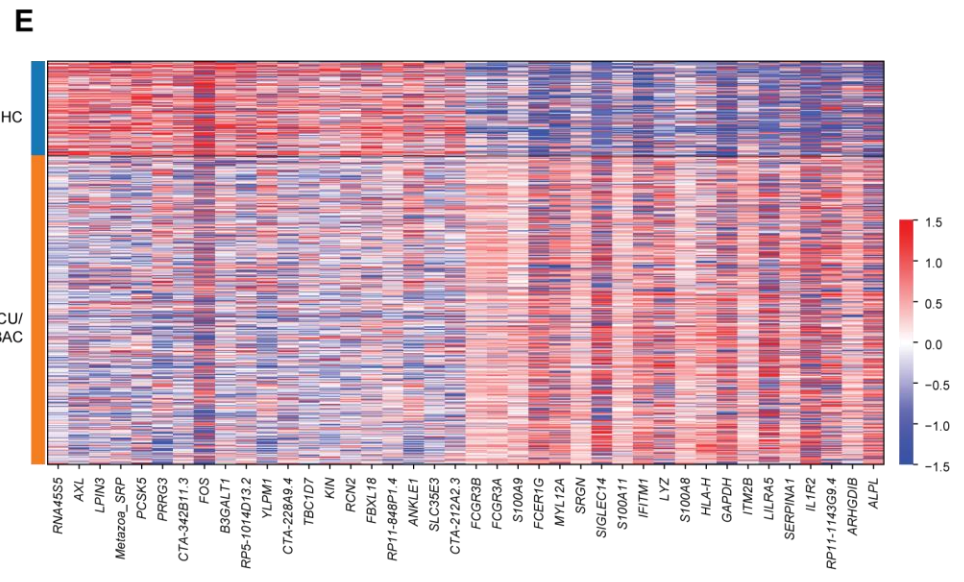
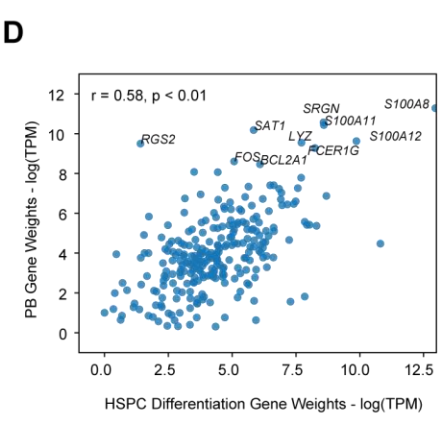
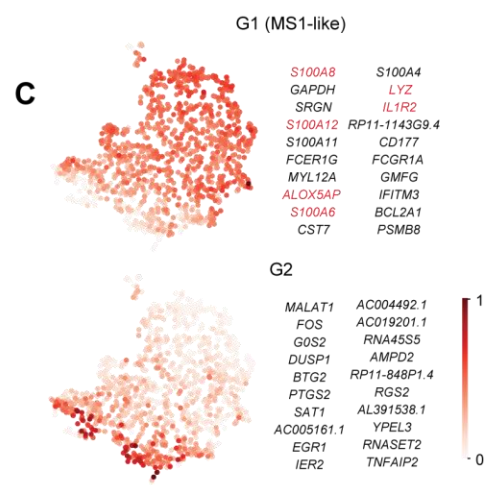
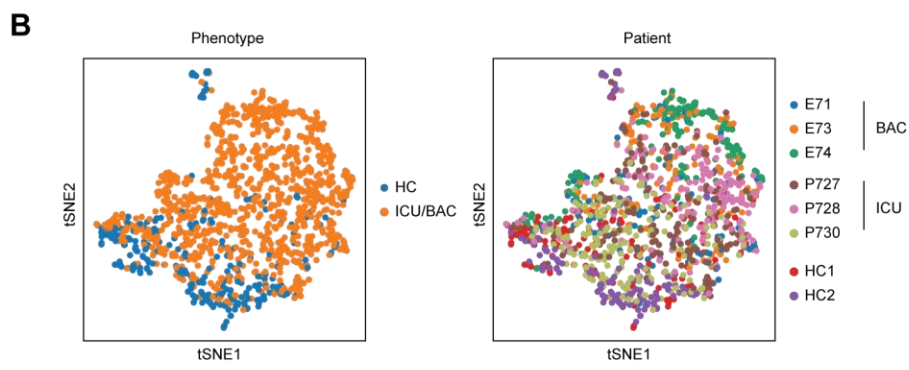
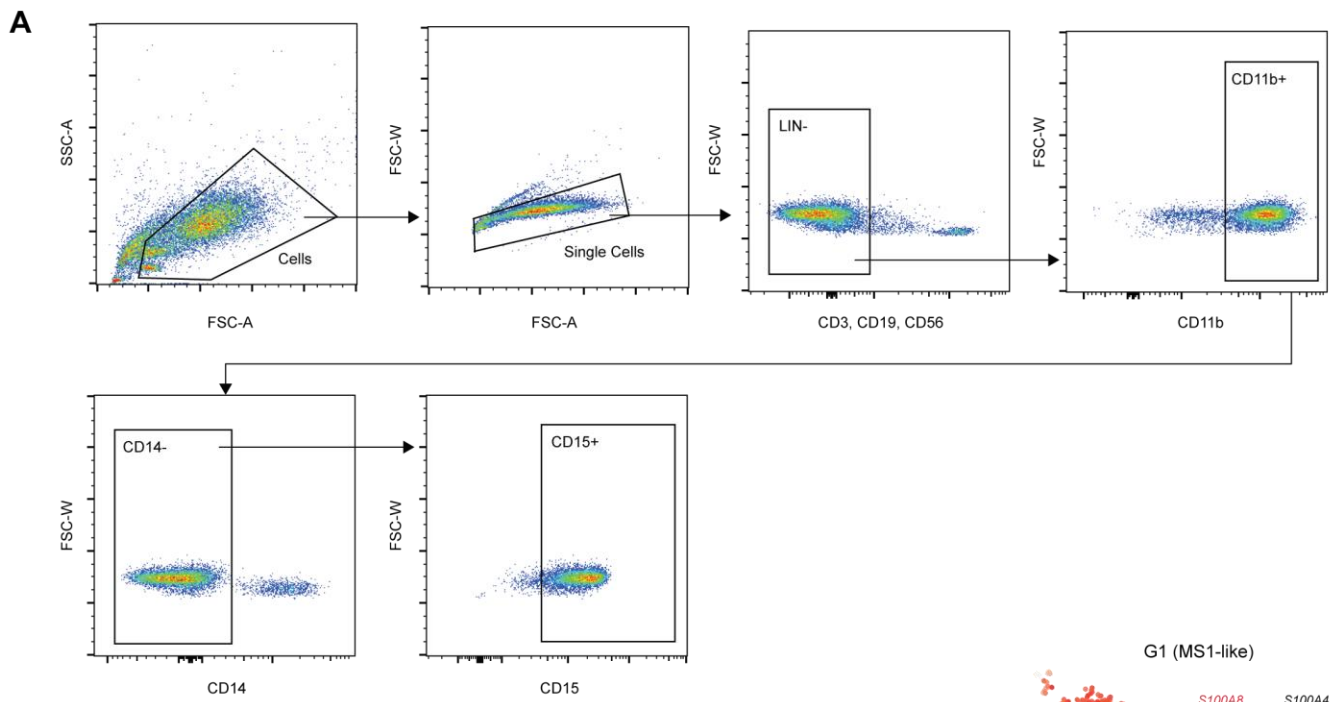


Figure S4. scRNA-seq of neutrophils sorted from critically-ill and bacteremic patients. (A) Gating strategy for single cell sorting of neutrophils. (B) tSNE plot ($n = 2,168$ cells) of neutrophil scRNA-seq data colored by cohort (left) and individual patients (right). (C) Relative usage of two gene modules unbiasedly derived from the neutrophil data (by cNMF). The top 20 genes in each module are listed. Genes in module N1 that are also among the top 30 genes in the MS1 module are highlighted in red. (D) Gene weight correlation between the MS1-like modules detected in neutrophils generated from incubation of HSPCs with sepsis plasma (x-axis) and neutrophils isolated from sepsis patients (y-axis). Significance of the correlations (Pearson r) are calculated with a permutation test. (E) Heatmap showing the top 20 differentially expressed genes (Wilcoxon rank-sum test, FDR < 0.01) between neutrophils sorted from critically-ill patients and healthy controls. BAC, bacteraemic patient; ICU, patient in intensive care.

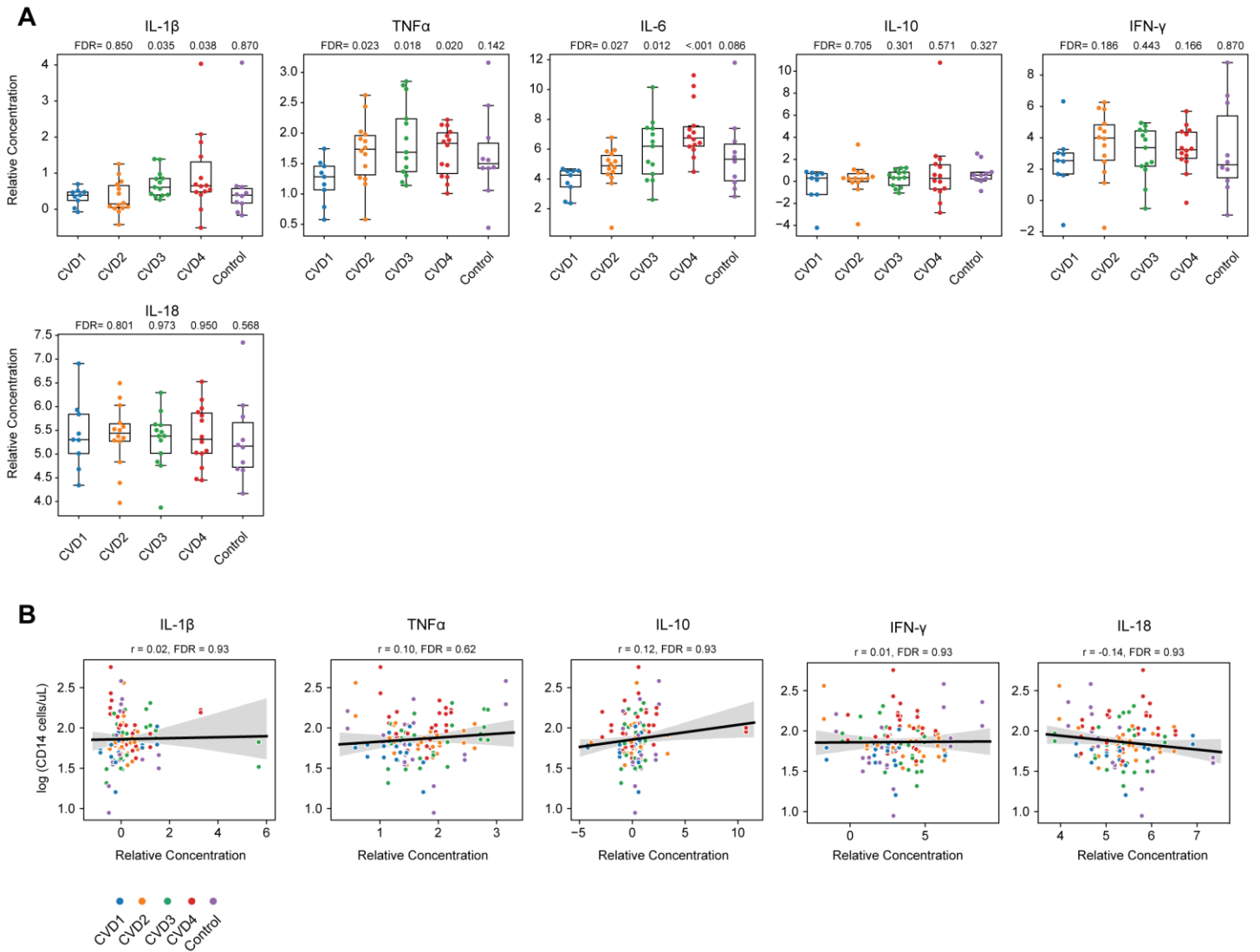


Figure S5. Plasma inflammatory cytokine levels in COVID-19 patients and correlation with cellular output. (A) Boxplots showing NPX (normalized protein expression) levels of inflammatory cytokines in plasma for each patient ($n = 61$). FDR values are shown when comparing each disease state with healthy controls (two-tailed Wilcoxon rank-sum test, corrected for testing of multiple cytokines). Boxes show the median and IQR for each patient cohort, with whiskers extending to 1.5 IQR in either direction from the top or bottom quartile. (B) Correlation between cytokine levels and CD14 cell output after CD34+ HSPCs are incubated with plasma for 7 days. Line and shadow indicate linear regression fit and 95% confidence interval, respectively. Significance of the correlations (Pearson r) were calculated with a two-sided permutation test.

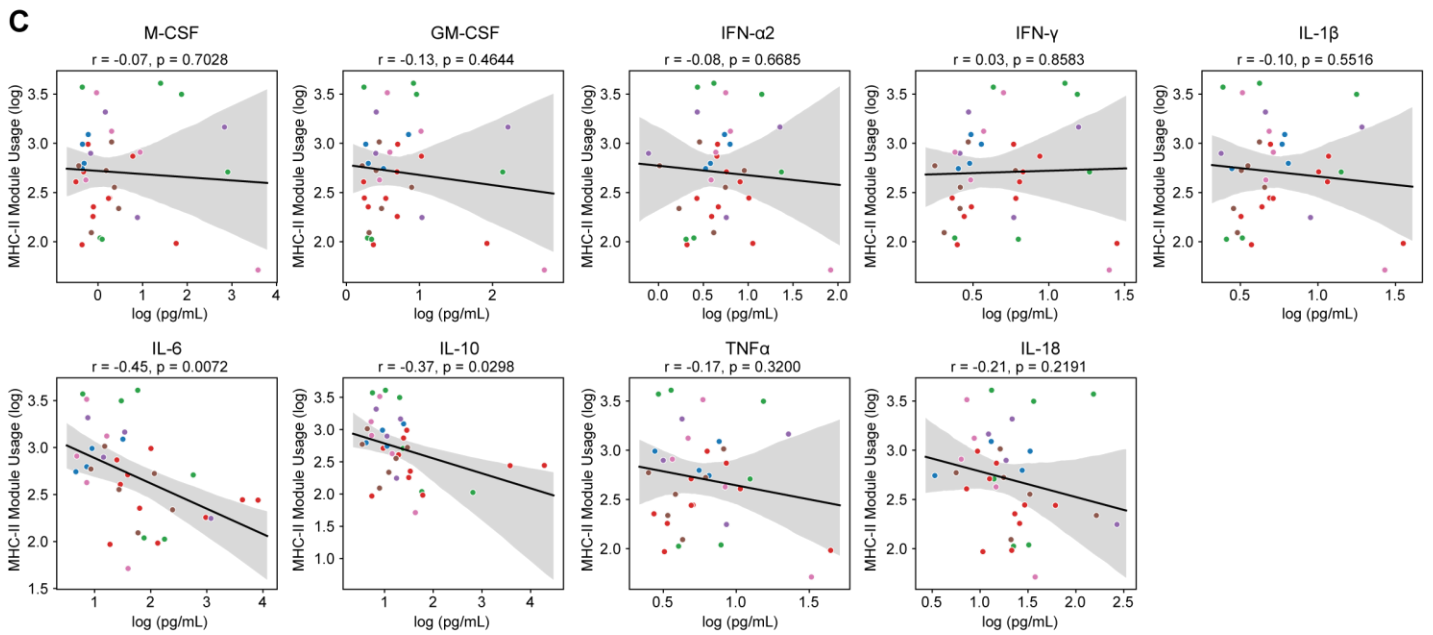
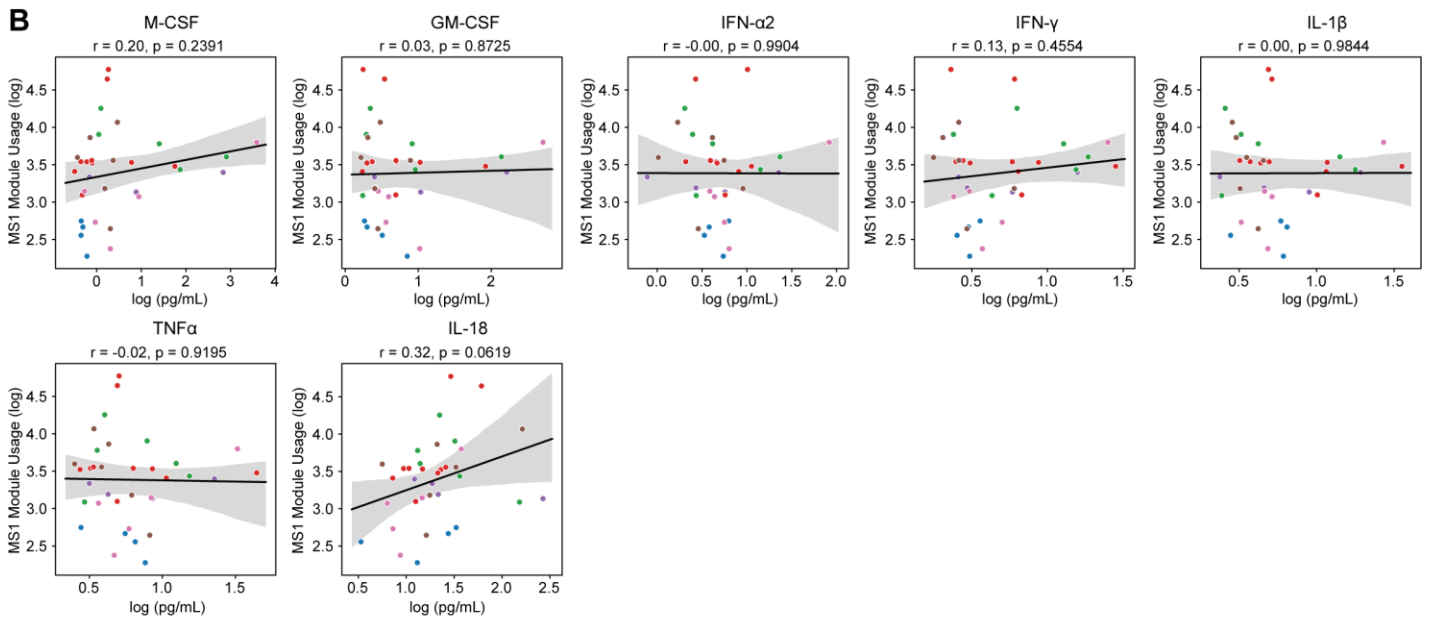
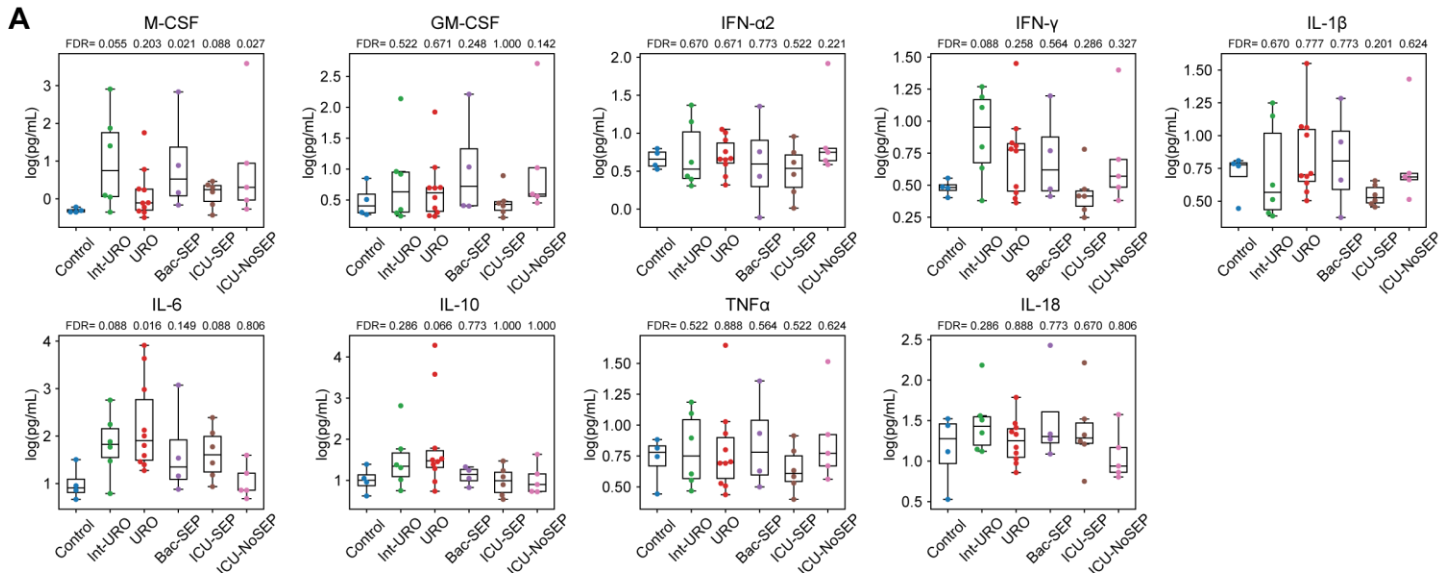


Figure S6. Plasma inflammatory cytokine levels in sepsis patients and correlations with monocyte gene expression modules. (A) Boxplots showing levels of indicated inflammatory cytokines in plasma for each patient ($n = 40$ total). FDR values are shown when comparing each disease state with healthy controls (two-tailed Wilcoxon rank-sum test, corrected for testing of multiple cytokines). Boxes show the median and IQR for each patient cohort, with whiskers extending to 1.5 IQR in either direction from the top or bottom quartile. (B-C) Correlations between level of each indicated cytokine and MS1 (B) or MHC-II (C) module usage in each patient ($n = 40$ total). Line and shadow indicate linear regression fit and 95% confidence interval, respectively. Significance of the correlations (Pearson r) were calculated with a two-sided permutation test.

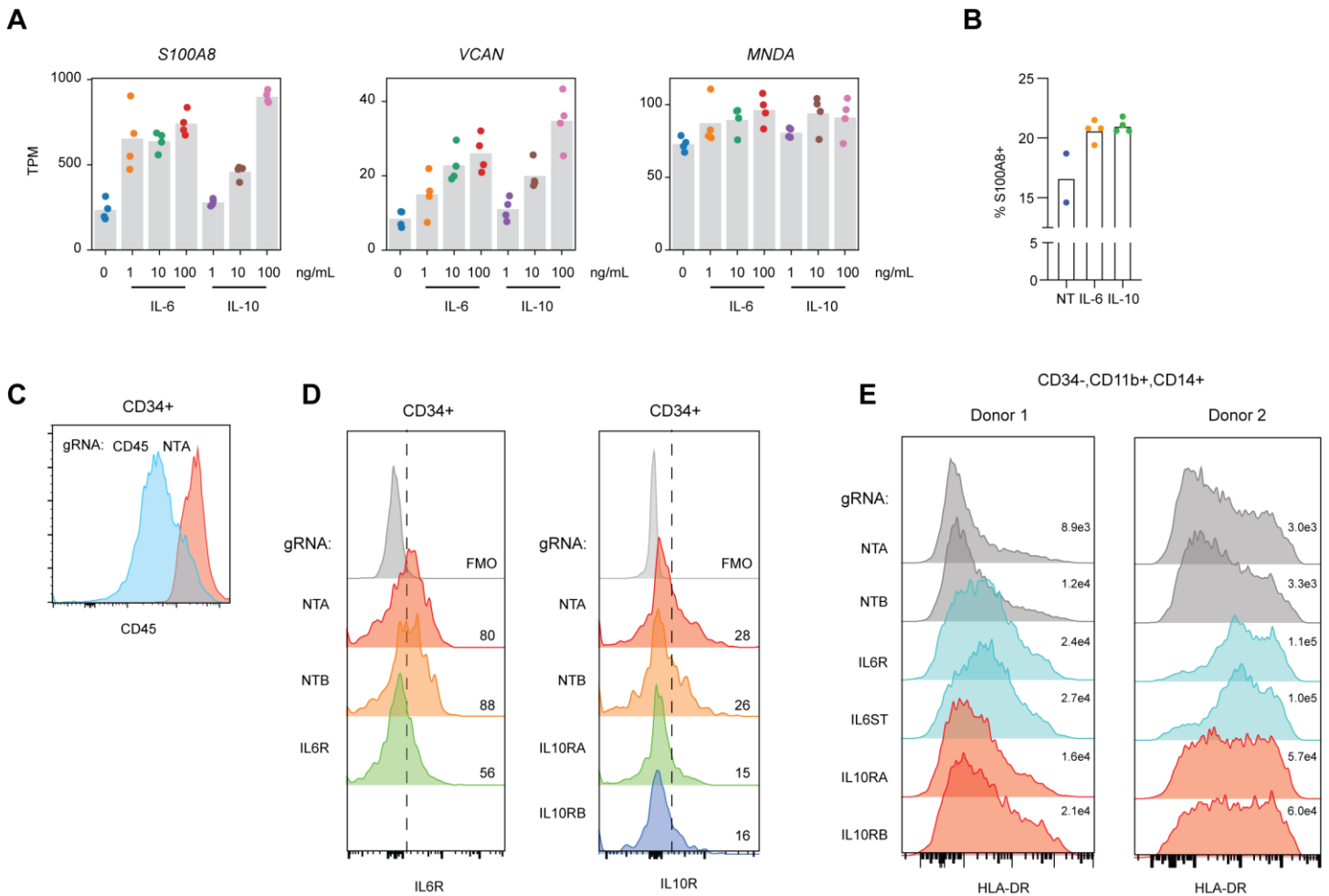


Figure S7. Short term stimulation and Cas9 RNP-based knockouts of CD34+ HSPCs. (A) Expression of 'early' MS1 genes in CD34+ HSPCs after treatment with IL-6 or IL-10 for 24 h. Experiments were performed with $n = 4$ for each condition (2 bone marrow donors with 2 technical replicates). (B) S100A8 intracellular staining of CD34+ HSPCs treated with 100 ng/mL IL-6 or IL-10 for 24 h. (C) CD45 surface expression levels in CD34+ HSPCs electroporated with either CD45 or NTA RNPs. (D) IL6R (left) and IL10R (right) expression in CD34+ HSPCs electroporated with the indicated gRNA-RNPs. Numbers indicate the percentage of cells that are IL6R+ or IL10R+, determined by gating on the full-minus-one (FMO) control. Results are representative of 2 independent experiments in different bone marrow donors. (E) Expression of HLA-DR in CD14+ cells after differentiation of RNP-electroporation HSPCs with 20% sepsis plasma for 2 bone marrow donors. Median fluorescence intensities are indicated for each sample.

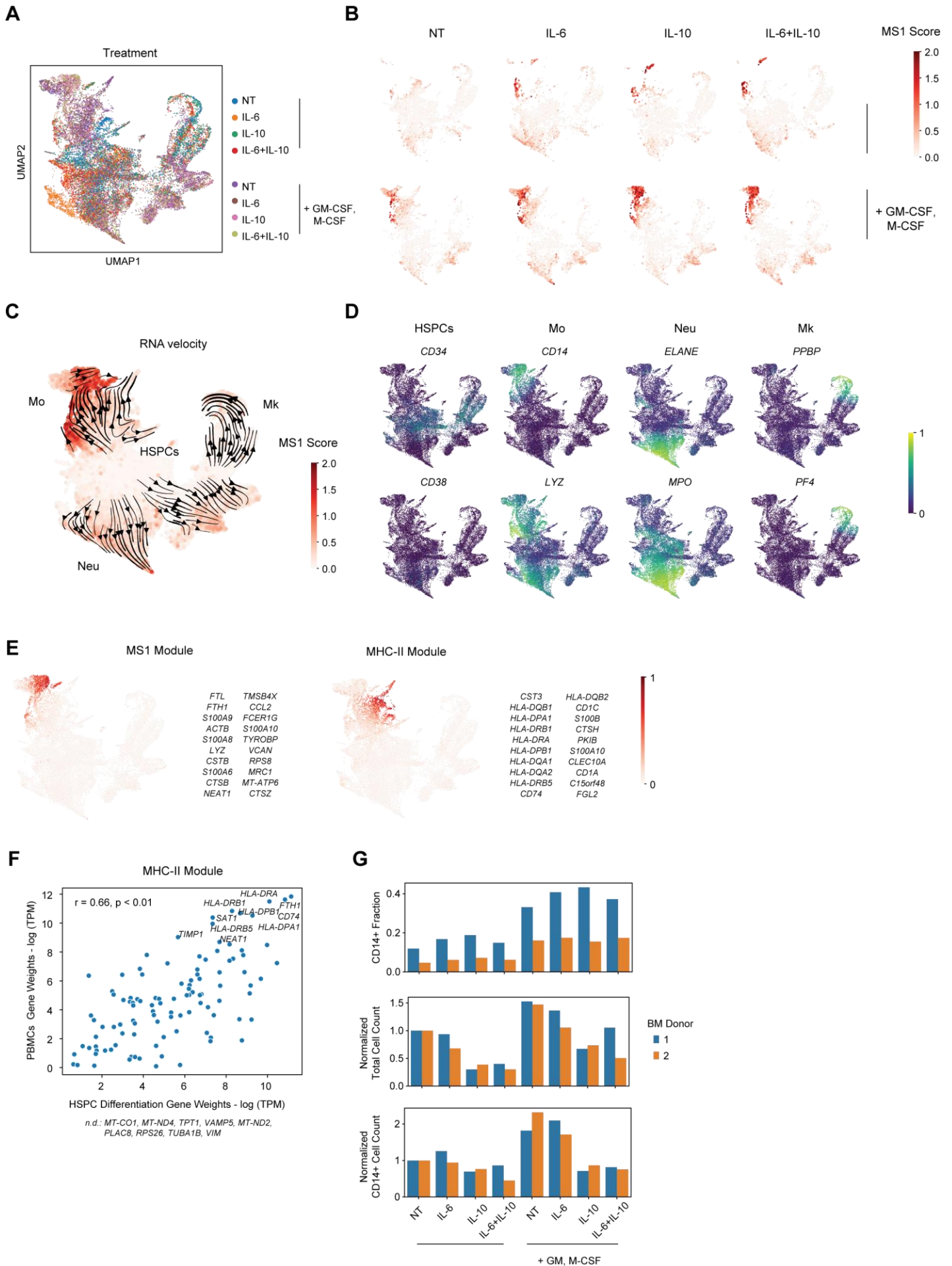


Figure S8. scRNA-seq of cytokine-differentiated HSPCs. (A) UMAP projection of differentiated cells from CD34+ HSPCs incubated with cytokines (all at 100 ng/mL). Cells are colored by cytokine conditions. (B) Individual UMAP projections of each cytokine condition with cells colored by MS1 scores. (C) Combined UMAP projection of all cytokine conditions with cells colored by MS1 scores. Stream plots showing inferred trajectories from RNA velocity are overlaid. Mo, monocytes; Neu, neutrophils; Mk, megakaryocytes. (D) Relative expression of HSPC, monocyte, neutrophil, and megakaryocyte marker genes in (A). (E) Relative expression of the MS1 and MHC-II modules. The top 20 genes in each module are listed. (F) Gene weight correlation between the MHC-II modules detected in the cytokine treatment (x-axis) and patient PBMC datasets (y-axis). Significance of the Pearson correlation (r) is calculated with a permutation test. Genes which are not detected (n.d.) in the cytokine treatment module but are among the top 30 for the corresponding module in the PBMC dataset are indicated. (G) Fraction of CD14+ cells (top), total number of cells (middle), and total number of CD14+ cells (bottom) after incubation of HSPCs in the indication cytokines. Cell counts were normalized to the NT condition (without GM/M-CSF) for each bone marrow donor. The experiment was performed on 2 bone marrow donors for each treatment condition; a total of 3,365, 2,986, 2,550, 3,025, 3,194, 3,061, 2,850, and 2,918 cells for each cytokine treatment condition indicated on the plots, respectively, were profiled.

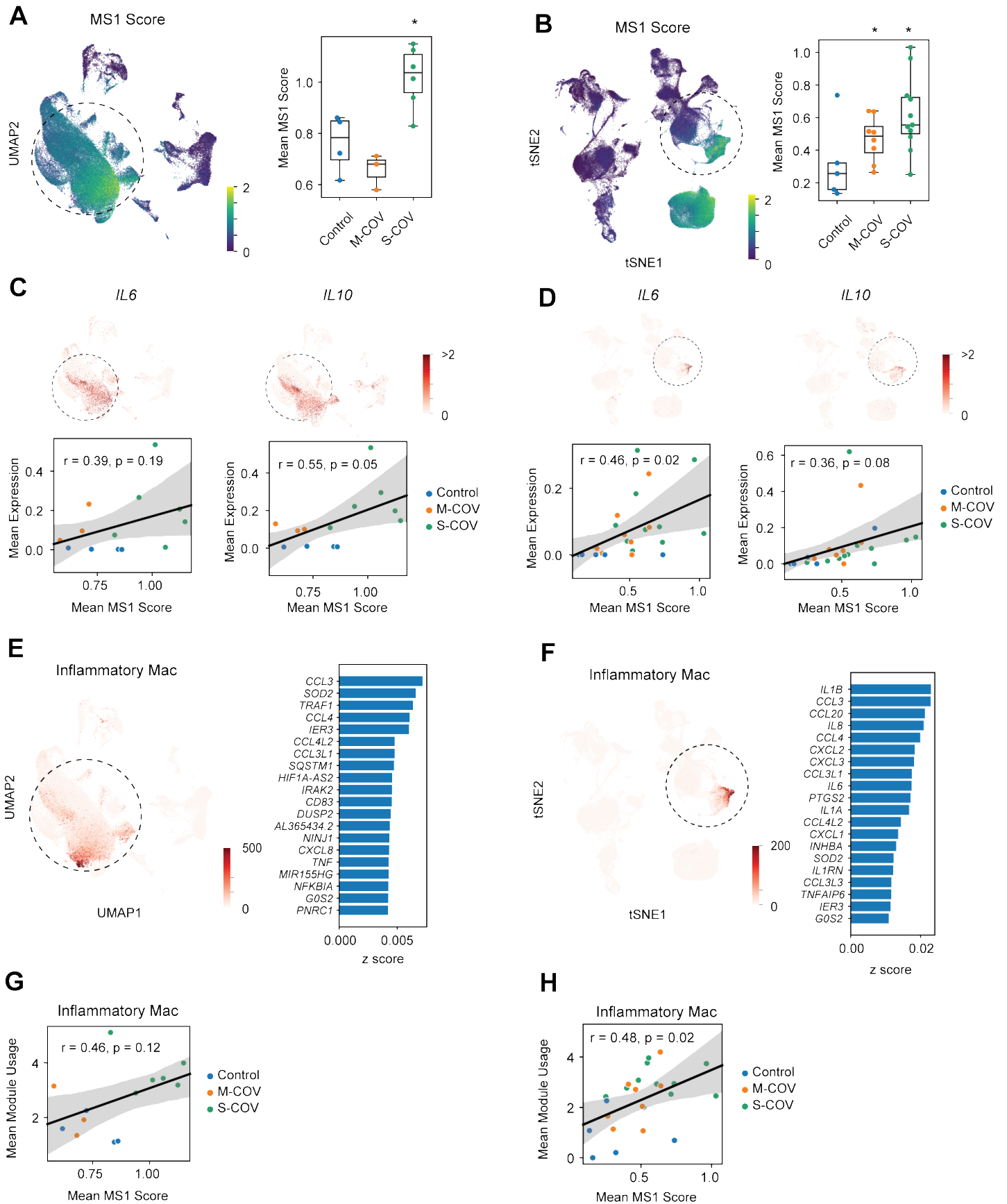


Figure S9. Expression of the MS1 program in tissues is associated with inflammatory macrophage activation. Single cell gene expression analysis of bronchoalveolar lavage fluid (BALF) and nasopharyngeal swabs (NS) from published COVID-19 datasets (44, 45). **(A,B)** UMAP/tSNE projection of cells colored by MS1 score. MS1 scores were calculated based on the top 30 genes from the MS1 module. The clusters corresponding to monocytes/macrophages are indicated by a dotted circle. Mean MS1 scores in monocytes/macrophages for each patient across patient groups for each dataset are shown on the right. Asterisks indicate $p < 0.05$, computed by comparing each disease state with healthy controls (two-tailed Wilcoxon rank-sum test). Boxes show the median and IQR for each patient cohort, with whiskers extending to 1.5 IQR in either direction from the top or bottom quartile. **(C,D)** UMAP/tSNE projection (top) of cells colored by expression of *IL6* (left) or *IL10* (right). Scatterplots (bottom) showing the correlation between mean expression of *IL6* (left) or *IL10* (right) with MS1 scores in each patient. Line and shadow indicate linear regression fit and 95% confidence interval, respectively. Significance of the correlation (Pearson r) was calculated with a two-sided permutation test. **(E,F)** UMAP/tSNE projection of cells colored by expression of an inflammatory macrophage module detected by cNMF. Genes with the top 10 loadings in the inflammatory macrophage module are shown on the right. **(G,H)** Correlation between mean expression of *IL6* (left) or *IL10* (right) with MS1 scores in each patient.

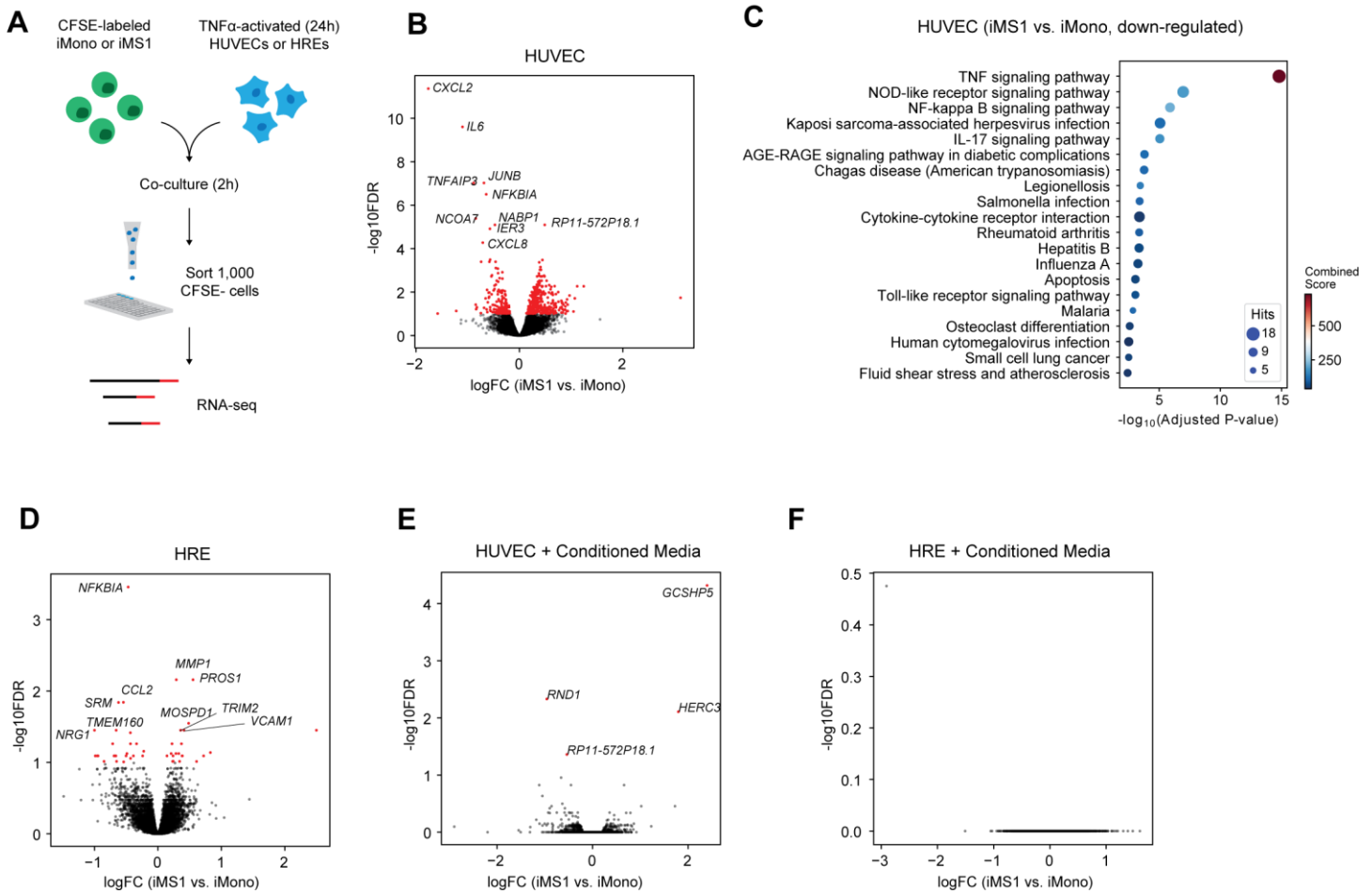


Figure S10. iMS1 co-incubation experiments with structural cells. (A) Experimental schematic of the co-incubation of iMS1 or iMono with primary human umbilical vein endothelial cells (HUVECs) or human renal epithelial cells (HREs). (B) Volcano plot showing differential expression analysis results (exact test) between TNF α -activated HUVECs co-incubated with either iMono or iMS1 cells generated from CD34+ HSPCs. Genes with FDR < 0.1 are highlighted in red, and the top 10 genes with lowest FDR values are shown. (C) Dotplot showing enrichment of pathways (KEGG database) for down-regulated genes in HUVECs co-incubated with iMS1 vs. iMono (FDR < 0.1, edgeR exact test). Sizes of circles are proportional to the number of gene hits in a set, whereas color represents the enrichment score of each gene set. (D) Volcano plot showing differential expression analysis results (exact test) between TNF α -activated HREs co-incubated with either iMono or iMS1 cells generated from CD34+ HSPCs. Genes with FDR < 0.1 are highlighted in red, and the top 10 genes with lowest FDR values are shown. (E-F) Volcano plot showing differential expression analysis results (exact test) between TNF α -activated HUVECs (E) or HREs (F) incubated with iMono or iMS1 conditioned media. Genes with FDR < 0.1 are highlighted in red. In (B-D) and (E-F), $n = 8$ experiments were performed for each condition (2 bone marrow donors with 2 biological and 2 technical replicates)

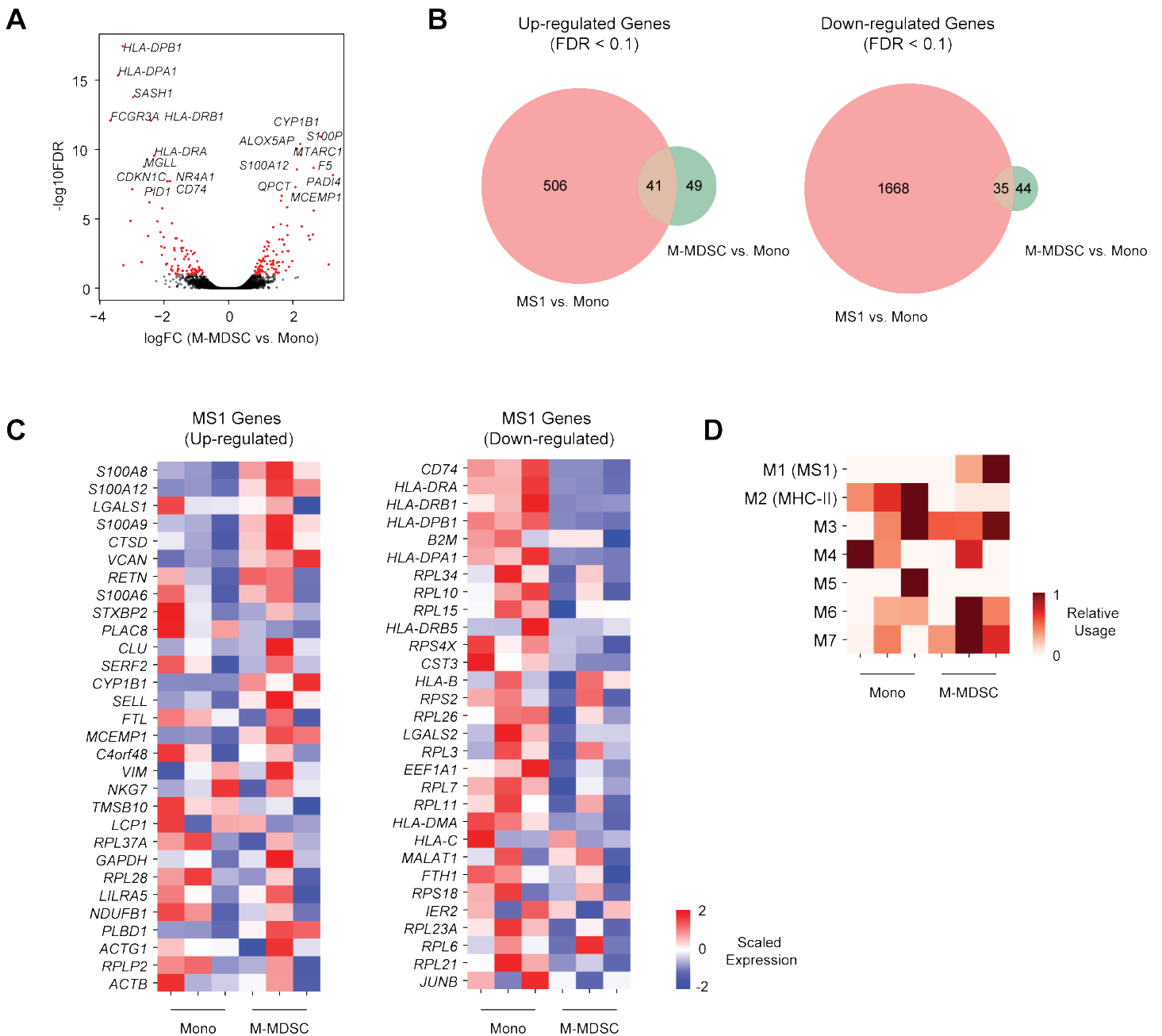


Figure S11. Comparison of MS1 with M-MDSCs. (A) Volcano plot showing differential expression analysis results (exact test) between M-MDSCs and monocytes ($n = 3$ for each) in lung cancer patients from Mastio, *et al* (54). Genes with $FDR < 0.1$ are highlighted in red. (B) Venn diagrams showing overlap of differentially expressed genes ($FDR < 0.1$, exact test) for MS1 vs. monocytes and M-MDSCs vs. monocytes. (C) Heatmaps showing the expression of the top 30 up-regulated (left) or down-regulated (right) MS1 genes in bulk RNA-seq of monocytes and M-MDSCs ($n = 3$ patients for each). (D) Relative usage of monocyte modules in monocytes and M-MDSCs.